

ARTICLE OPEN



LYMPHOMA

Pharmacologic targeting of Nedd8-activating enzyme reinvigorates T-cell responses in lymphoid neoplasia

Xiaoguang Wang^{1,7}, Canping Chen^{2,7}, Dan Vuong¹, Sonia Rodriguez-Rodriguez¹, Vi Lam¹, Carly Roleder¹, Jing H. Wang³, Swetha Kambhampati¹, Allison Berger⁴, Nathan Pennock⁵, Pallawi Torke⁶, Francisco Hernandez-Ilizaliturri⁶, Tanya Siddiqi¹, Lili Wang¹, Zheng Xia² and Alexey V. Danilov¹✉

© The Author(s) 2023

Neddylation is a sequential enzyme-based process which regulates the function of E3 Cullin-RING ligase (CRL) and thus degradation of substrate proteins. Here we show that CD8⁺ T cells are a direct target for therapeutically relevant anti-lymphoma activity of pevonedistat, a Nedd8-activating enzyme (NAE) inhibitor. Pevonedistat-treated patient-derived CD8⁺ T cells upregulated TNF α and IFN γ and exhibited enhanced cytotoxicity. Pevonedistat induced CD8⁺ T-cell inflamed microenvironment and delayed tumor progression in A20 syngeneic lymphoma model. This anti-tumor effect lessened when CD8⁺ T cells lost the ability to engage tumors through MHC class I interactions, achieved either through CD8⁺ T-cell depletion or genetic knockout of *B2M*. Meanwhile, loss of *UBE2M* in tumor did not alter efficacy of pevonedistat. Concurrent blockade of NAE and PD-1 led to enhanced tumor immune infiltration, T-cell activation and chemokine expression and synergistically restricted tumor growth. shRNA-mediated knockdown of HIF-1 α , a CRL substrate, abrogated the in vitro effects of pevonedistat, suggesting that NAE inhibition modulates T-cell function in HIF-1 α -dependent manner. scRNA-Seq-based clinical analyses in lymphoma patients receiving pevonedistat therapy demonstrated upregulation of interferon response signatures in immune cells. Thus, targeting NAE enhances the inflammatory T-cell state, providing rationale for checkpoint blockade-based combination therapy.

Leukemia (2023) 37:1324–1335; <https://doi.org/10.1038/s41375-023-01889-x>

INTRODUCTION

Immunotherapy revolutionized cancer care: immune checkpoint inhibitors received FDA approvals for treatment of multiple tumor types, and cell-based therapies (i.e., chimeric antigen receptor T cells) transformed standard of care of patients with non-Hodgkin lymphoma (NHL) and acute lymphoblastic leukemia. More recently, bi-specific T-cell engagers have shown impressive clinical activity in hematologic malignancies [1]. While such strategies are highly effective, they remain non-curative and novel approaches to enhance their clinical impact are necessary.

Contrary to chemotherapy, novel targeted therapies are associated with diverse immunomodulatory effects [2, 3]. For example, inhibitors of B-cell receptor-associated kinases, now widely used in therapy of NHL, may enhance T-cell function through multiple mechanisms, including reversal of exhaustion, altered T-cell polarization, and neutralization of the immunosuppressive effect by the neoplastic cells [3, 4]. Importantly, the clinical efficacy of compounds which target protein degradation, such as the E3 ubiquitin ligase modulator lenalidomide, in large part depends on their immunomodulatory effects [5, 6]. Thus, investigation of pathways within the

ubiquitin-proteasome system (UPS) which may be engaged to enhance anti-tumor immunity is of critical importance.

Cullin-RING E3 ubiquitin ligases (CRLs) conjugate ubiquitin chains to unwanted or misfolded proteins in cells, eventually leading to proteasome-mediated degradation [7]. To undergo the conformational change and enable substrate ubiquitination, the CRLs require conjugation of the active ubiquitin-like protein NEDD8 to the scaffold Cullin proteins, a process referred to as neddylation [8]. Like ubiquitination, neddylation is a three-step sequential enzymatic reaction which starts with NEDD8 activation by the E1 NEDD8-activating enzyme (NAE, NAE1/UBA3 heterodimer), followed by NEDD8 transfer to the E2 NEDD8-conjugating enzymes (UBC12 and UBE2F) and finally NEDD8 addition to the Cullin proteins [9].

Pevonedistat (MLN4924, TAK924) is a small molecule that covalently adducts with NEDD8, rendering it inactive and eventually leading to CRL deactivation and accumulation of CRL-dependent substrates [10]. Targeting neddylation with pevonedistat demonstrated preclinical and early clinical efficacy across a spectrum of hematologic malignancies and solid tumor types, alone and in combination with chemotherapeutic, hormonal and

¹City of Hope National Medical Center, Duarte, CA, USA. ²Computational Biology Program, Department of Biomedical Engineering, Oregon Health & Science University, Portland, OR, USA. ³Department of Medicine, Division of Hematology/Oncology, University of Pittsburgh, Pittsburgh, PA, USA. ⁴Takeda Development Center Americas, Cambridge, MA, USA. ⁵Knight Cancer Institute, Oregon Health & Science University, Portland, OR, USA. ⁶Division of Hematology & Medical Oncology, Roswell Park Cancer Institute, Buffalo, NY, USA. ⁷These authors contributed equally: Xiaoguang Wang, Canping Chen. ✉email: adanilov@coh.org

Received: 3 October 2022 Revised: 22 March 2023 Accepted: 24 March 2023

Published online: 8 April 2023

targeted agents [10–20]. On the other hand, neddylation has been implicated in regulation of immune cell function [21–23]. Our group first demonstrated that pharmacologic targeting NAE rehabilitated T cells derived from patients with chronic lymphocytic leukemia (CLL), leading to decreased Treg differentiation and enhanced T_H1 polarization, accompanied by increased production of interferon- γ (IFN- γ), and confirmed these findings in immunized mice [21]. However, whether altering neddylation may ultimately enhance anti-tumor immunity, and contribute to the direct anti-tumor effects of pevonedistat in lymphoma and other cancers, remains unknown. In the current work, we employed the A20 syngeneic lymphoma mouse model and primary samples from patients treated with pevonedistat to demonstrate that targeting neddylation directly enhances anti-tumor response by promoting T-cell activation.

METHODS

Patient samples

Following approval by the Institutional Review Board and provision of written informed consent, peripheral blood was obtained from CLL patients treated at City of Hope National Medical Center (Duarte, CA). Peripheral blood samples were obtained from eight patients with NHL and CLL who received pevonedistat on a Phase I clinical trial (at baseline, 3 and 24 h after pevonedistat infusion; Supplementary Table S1; NCT03479268) [24]. Peripheral blood mononuclear cells (PBMCs) were isolated using standard Ficoll-Hypaque technique (Amersham). Red blood cells were lysed using ACK buffer (Thermo Fisher Scientific).

Cell culture

A20, JeKo-1, Mino, Val, Maver-1 and Lewis lung carcinoma (LLC) cells were obtained from American Type Culture Collection (ATCC, USA). Mycoplasma testing was performed regularly (every 2 months) using Mycoplasma PCR detection kit (ABM, Canada). The number of passages between thawing and use in the described experiments ranged between two and five. Cells were cultured in RPMI-1640 medium supplemented with 15% fetal bovine serum, 100 U/mL penicillin, 100 μ g/mL streptomycin, 2 mM L-glutamine, 25 mM HEPES, 100 μ M nonessential amino acids, and 1 mM sodium pyruvate (Lonza).

Total $CD3^+$ T cells were isolated from PBMCs derived from CLL patients by positive selection kit (Invitrogen, USA) and cultured with 0.5 μ g/mL plate-bound anti-CD3 (clone UCHT1) and 0.5 μ g/mL soluble anti-CD28 (clone CD28.2; BD Biosciences).

Pevonedistat (TAK924) was provided by Takeda Development Center Americas, Inc.

Cell viability testing

To measure cell proliferation, cells were plated in 96-wellplates (5000 cells/well, 3 wells/sample) with drugs and incubated for 48 h at 37 °C in 5% CO_2 . After incubation, relative numbers of viable cells were measured using a tetrazolium-based colorimetric assay (CellTiter Aqueous One Solution Cell Proliferation Assay, Promega).

For cytotoxicity assay, stimulated T cells were harvested and washed three times with PBS. Lymphoma cells were labeled with CFSE and co-cultured with T cells in 1:1 or 5:1 ratio for additional 48 h. Apoptosis was measured using the ApoScreen Annexin V Apoptosis Kit (Southern Biotech). Briefly, cells were resuspended in 100 μ L Annexin V binding buffer containing 0.5 μ L Annexin V mAb and 0.5 μ L 7-aminoactinomycin D (7-AAD). Cells were then subjected to flow cytometry and double-positive (Annexin V/&-AAD) population was analyzed.

Immunoblotting

Cells were lysed in RIPA buffer (20 mM Tris, 150 mM NaCl, 1% NP-40, 1 mM NaF, 1 mM sodium phosphate, 1 mM $NaVO_3$, 1 mM EDTA, 1 mM EGTA), supplemented with protease inhibitor cocktail (Roche), phosphatase inhibitor cocktail 2 (Sigma-Aldrich) and 1 mM phenylmethanesulfonyl fluoride. Primary antibodies used in Western blot analysis were listed in Supplementary Table S2. Secondary horseradish peroxidase-conjugated anti-mouse and anti-rabbit were purchased from Cell Signaling Technology. Protein bands were developed by ECL Western blotting detection reagents (GE Healthcare) according to kit instructions.

In vivo experiments

Six-to-eight-week-old mice were purchased from The Jackson Laboratory (United States). Mice were injected subcutaneously at both flanks with 1×10^6 A20 lymphoma cells (WT BALB/c) or LLC cells (WT C57BL/6 (B6)). When tumors reached 100 mm³, tumor-bearing recipient mice were randomized into groups and treated as indicated. All mice were maintained under specific pathogen-free conditions in the vivarium facility of City of Hope. Animal work was approved by the Institutional Animal Care and Use Committee of City of Hope. The following drugs were used: InVivoMAB anti-mouse CD8 α (clone 53-6.7), InVivoPlus anti-mouse PD-1 (clone RMP1-14; both from BioXCell).

Tumor dissociation and flow cytometry

Tumors were harvested from tumor-bearing mice. Tumor weight was measured before dissociation and tumors were processed into single-cell suspension. Antibodies used for flow cytometry were listed in Supplementary Table S2. For tumors and human PBMC cells, dead cells were excluded by Live/Dead fixable aqua dead cell stain kit (Invitrogen). BD Fix/Permeabilization buffer was used for intracellular staining of IFN- γ , TNF- α , IL-2, IL-4 and IL-17 in tumor-infiltrating lymphocytes (TILs).

For cytokine staining, equal numbers of tumor (or human PBMC cells) were cultured in vitro for 5 h in the presence of 50 ng/mL phorbol 12-myristate 13-acetate (PMA) (Sigma Aldrich), 1 μ g/mL ionomycin (Sigma Aldrich) and 5 μ g/mL BFA (Biolegend). For FoxP3 staining, True-nuclear Transcription Factor Buffer Set was used (Biolegend). Data were acquired on BD Fortessa and analyzed with FlowJo software V10 (Oregon, USA).

Statistical analysis

At least 3 biological replicates were used in all experiments shown throughout the manuscript, unless noted otherwise. Statistical analysis was performed with Student t test or one-way ANOVA with Tukey's multiple comparisons test, when indicated, in GraphPad Prism software. * $p < 0.05$, ** $p < 0.01$ and *** $p < 0.001$ throughout the manuscript. Research reported in this publication included work performed in the Hematopoietic Tissue Biorepository, the Integrative Genomics and Bioinformatics Core and the Analytical Cytometry Cores and supported by the National Cancer Institute of the National Institutes of Health under award number P30CA033572.

RESULTS

Pharmacologic targeting NAE enhances T-cell cytotoxicity in vitro

We have previously shown that NAE inhibition-induced IFN- γ and downmodulated IL-2 expression in primary $CD4^+$ T cells [21]. To investigate whether interference with the neddylation pathway altered the functionality of cytotoxic lymphocytes, primary T cells isolated from peripheral blood of CLL patients were subjected to TCR engagement followed by treatment with pevonedistat. We observed that NAE inhibition led to increased secretion of the effector molecules TNF- α and IFN- γ in human $CD8^+$ T cells (Fig. 1A; Supplementary Fig. 1A). By contrast, TNF- α expression and IFN- γ by $CD4^+$ T cells was unchanged. Microarray analysis of sorted naïve $CD3^+$ T cells has previously demonstrated mRNA transcript upregulation of the exhaustion markers following pevonedistat treatment [21]. Here we observed that CTLA-4 expression was induced by pevonedistat in both $CD8^+$ and $CD4^+$ T cells, while only $CD8^+$ T cells exhibited upregulation of PD-1 (Fig. 1B). Next, we evaluated the effect of pevonedistat on T-cell mediated cytotoxicity. While unstimulated patient-derived T cells failed to exhibit cytotoxicity, $CD3/28$ stimulation led to a significant killing of target lymphoma cells (Fig. 1C; Supplementary Fig. 1B). Pre-treatment with pevonedistat enhanced allogeneic T-cell-mediated killing of neoplastic B cells, suggesting that NAE inhibition may enhance cytotoxic cell function.

NAE inhibition activates tumor-infiltrating lymphocytes (TILs)

We had shown that NAE inhibition results in increased IFN- γ secretion and a reduction in T_{reg} population in ova immunization model, suggesting that NAE inhibition may modulate anti-tumor response in vivo [21]. To further explore the immunomodulatory

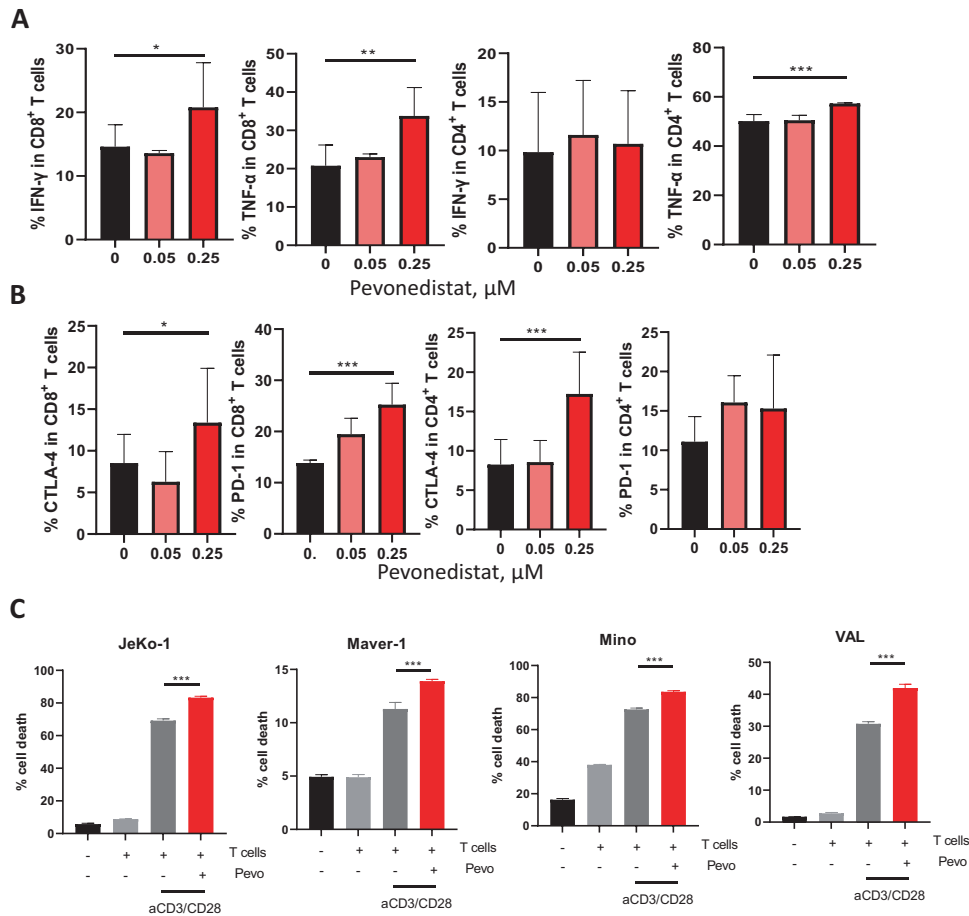


Fig. 1 NAEi modulates CD8 $^+$ T-cell response. Magnetically enriched CD3 $^+$ cells derived from patients with CLL ($n = 3$ individual patients) were activated with 0.5 $\mu\text{g}/\text{mL}$ $\alpha\text{CD3}/28$ for 24 h. Thereafter, stimulation continued in the presence of the indicated doses of pevonedistat or vehicle control for an additional 72 h. **A**, **B** Expression of IFN γ , TNF α , CTLA-4 and PD-1 was quantified in CD4 $^+$ or CD8 $^+$ T cells by flow cytometry. **C** T cells were treated as previously, followed by pevonedistat wash off. NHL cells were labeled with CFSE and co-cultured with T cells for additional 48 h. Cell death was quantified using Annexin V/7-AAD expression by flow cytometry. Data are mean \pm SD. One-way ANOVA was performed for statistical analysis, * $p < 0.05$, ** $p < 0.01$, *** $p < 0.001$.

effect of NAE inhibition in an immunocompetent model, A20 lymphoma cells were transplanted into syngeneic BALB/c mice. Tumors emerged approximately one week after inoculation. When tumor size reached $\sim 100 \text{ mm}^3$, mice were randomized into two groups and treated with either pevonedistat or vehicle control for 10 days (Fig. 2A). In this model, treatment with pevonedistat restricted tumor growth (Fig. 2B). Analysis of murine tumors at the end of treatment revealed that the absolute quantities of CD4 $^+$ and CD8 $^+$ TILs were significantly increased by pevonedistat (Fig. 2C; Supplementary Fig. 2). Furthermore, we observed an increased number of IFN- γ -producing CD8 $^+$ cells in tumors harvested from pevonedistat-treated mice compared with control animals (Fig. 2D). Meanwhile, treatment with pevonedistat had no effect on cytokine secretion by CD4 $^+$ cells (Fig. 2E). Expression of PD-1 was also unchanged in both T-cell subsets (Fig. 2D, E). Additionally, we did not observe a change in the infiltrating Treg cells (Fig. 2F).

To explore whether immunomodulation via NAE inhibition was restricted to the highly immunogenic A20 lymphoma model, we conducted experiments in Lewis lung carcinoma (LLC) which is considered a relatively immunologically cold tumor. Still, treatment with pevonedistat restricted growth of LLC tumors (Supplementary Fig. 3A). Interestingly, here we also observed a dramatic increase in both CD4 $^+$ and CD8 $^+$ TILs, albeit the absolute lymphocyte numbers were significantly lower than in the A20 model (Supplementary Fig. 3B). Furthermore, unlike in A20 model,

LLC TILs exhibited an increased expression of immune checkpoint molecules upon NAE inhibition (Supplementary Fig. 3C).

Thus, NAE inhibition modulated TILs in syngeneic mouse models.

CD8 $^+$ T cells are indispensable for the therapeutic effect of pevonedistat

We and others have shown that pevonedistat exerts direct anti-tumor effects across multiple tumor types [14, 16, 25–27]. Still, our findings strongly suggest that immune modulation significantly contributes to the therapeutic effect of pevonedistat. To further explore this, we first evaluated susceptibility of A20 cells to NAE inhibition in vitro. While pevonedistat is cytotoxic to multiple NHL cell lines, A20 cells were resistant to NAE inhibition (Fig. 3A, B) [26, 27]. To investigate the relative importance of TILs in pevonedistat-mediated anti-tumor effect, we used antibody-mediated depletion of CD8 $^+$ T cells in mice. Interestingly, loss of CD8 $^+$ T cells resulted in accelerated tumor growth, further implicating the immune environment in this mouse model (Fig. 3C). The therapeutic effect of NAE inhibition was also completely abrogated in lymphoma-bearing mice treated with anti-CD8 antibody. Consistent with our earlier data, the absolute numbers of both CD8 $^+$ TILs and IFN- γ -producing CD8 $^+$ cells were significantly increased by pevonedistat treatment, while expression of PD-1 remained unchanged (Fig. 3D; Supplementary Fig. 4A). As expected, CD8 $^+$ TILs were not detected in mice treated with anti-CD8 antibody, while the phenotypic and compositional

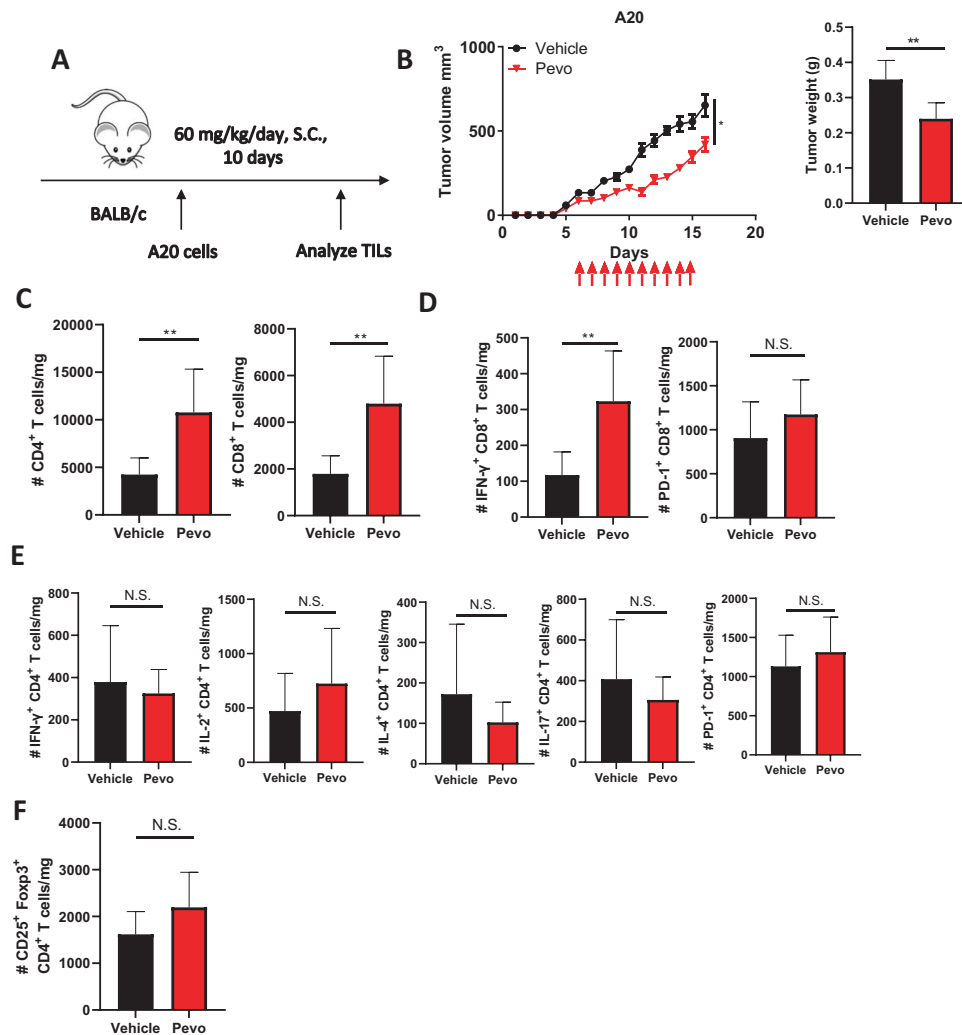


Fig. 2 Pevonedistat inhibits A20 tumor progression and modulates TILs. **A** A20 lymphoma cells were transplanted subcutaneously into syngeneic recipient mice. Mice were treated with pevonedistat 60 mg/kg for 10 days or vehicle control ($n = 6$ per group). Tumors were harvested on day 16 after inoculation and subsequently used for TIL analysis. **B** Tumors were measured every other day; tumor volumes at day 16 are shown on the right. **C–F** Immune profiles of CD4⁺ and CD8⁺ TILs assayed at the end of the experiment. Data are mean \pm SD. One-way ANOVA was performed for statistical analysis, * $p < 0.05$, ** $p < 0.01$.

profiles of the CD4⁺ T cells were unaffected (Fig. 3D, E; Supplementary Fig. 4B).

Since cytotoxic T cells require MHC class I molecules for antigen presentation, we explored whether their loss impacts pevonedistat efficacy. We had previously employed the CRISPR/Cas9 technique to generate knockout of $\beta 2$ -microglobulin (*B2M*-KO) [28]. The *B2M* knockout completely abolished the expression of MHC class I in A20 cells (Fig. 3F). While *B2M* loss did not negatively impact tumor growth either in vitro or in vivo, the anti-tumor effect of pevonedistat was fully abrogated (Fig. 3G). *B2M*-KO tumors did not attract TILs whose profiles from pevonedistat-treated mice were comparable with control animals (Fig. 3H; Supplementary Fig. 3C, D).

To further investigate the exact contribution of NAE inhibition in the tumor, we employed shRNA-mediated knockdown of *UBE2M* in A20 cells. *UBE2M*, encoded by *UBE2M*, is NEDD8-conjugating enzyme which governs neddylation [23]. *shUBE2M* A20 cells were transplanted into flanks of syngeneic BALB/c mice followed by pevonedistat treatment. We confirmed durability of *UBE2M* knockdown in transplanted A20 tumors (Fig. 4A). Surprisingly, we found that the therapeutic effect of pevonedistat was not altered by the intratumoral loss of *UBE2M* (Fig. 4B). Furthermore, TILs from pevonedistat-treated

mice whose tumors lacked *UBE2M* exhibited the same functional features as TILs in control mice (Fig. 4C, D; Supplementary Fig. 5).

Taken together, our data strongly implicate CD8⁺ T cells as a mediator of the anti-tumor effect of NAE inhibition.

HIF1A mediates NAE inhibition-induced anti-tumor immunity

The mechanism of neddylation-mediated immune regulation is understudied. CRL substrates which accumulate following blockade of NAE enzymatic activity may mediate immune effects. Among these substrates, GATA3 and HIF-1 α have been shown to modulate expression of immune checkpoint molecules and cytokine secretion by immune cells [29–31]. Hence, they were further investigated here. Treatment with pevonedistat led to accumulation of HIF-1 α in TCR-stimulated primary patient-derived T cells in vitro (Fig. 5A). By contrast, we observed a dose-dependent downregulation of GATA3 following pevonedistat exposure of human T cells. We next generated *HIF1A* knockdown in primary patient-derived T cells (Fig. 5B). Unlike control cells, CD4⁺/CD8⁺ human T cells which lacked HIF-1 α failed to upregulate checkpoint molecules and secrete cytokines upon treatment with pevonedistat in vitro (Fig. 5C, Supplementary Fig. 6). Furthermore, loss of HIF-1 α partially abrogated NAE

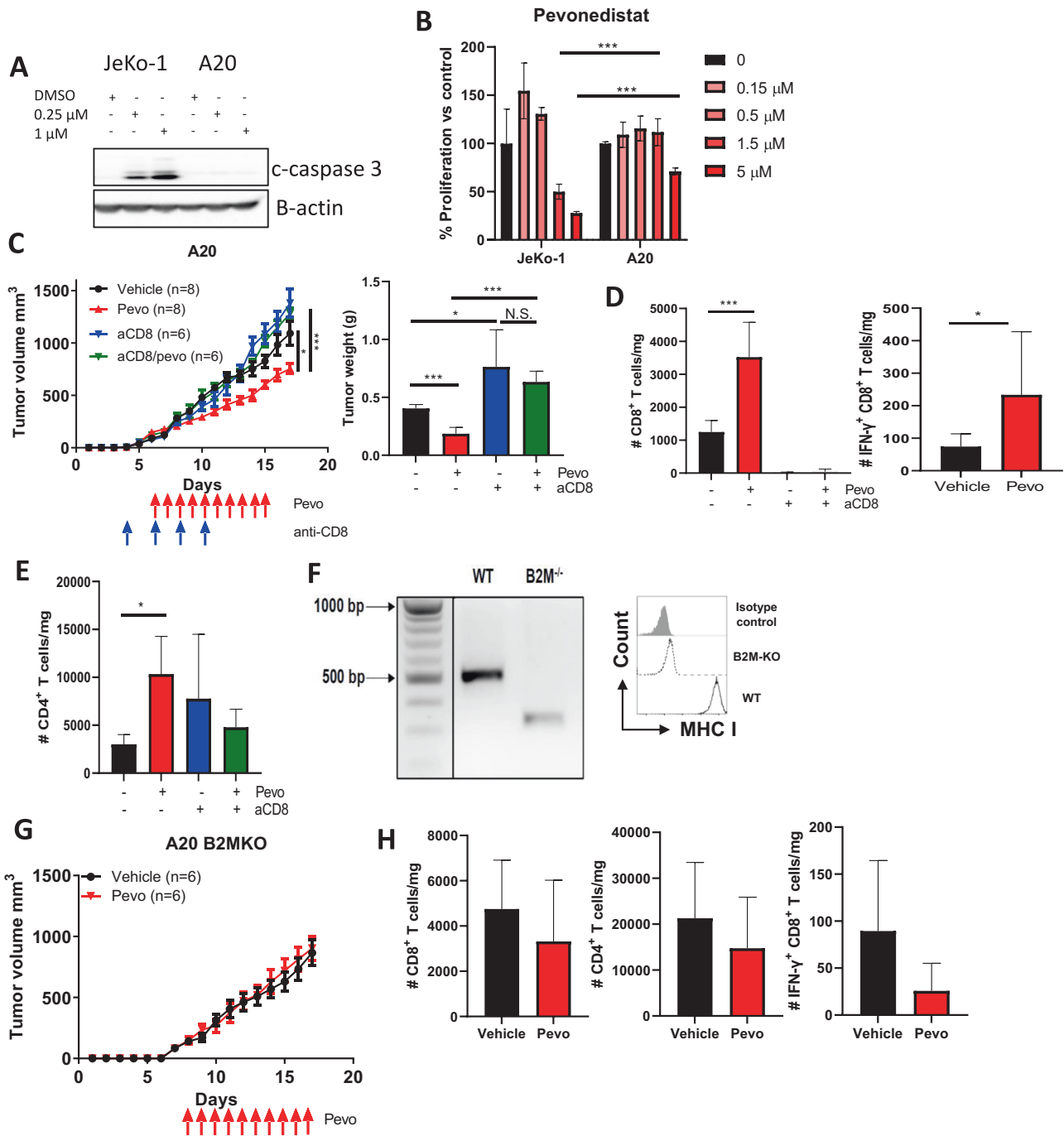


Fig. 3 Therapeutic effect of pevonedistat depends on CD8⁺ T cells. **A** A20 cells were treated with the indicated concentrations of pevonedistat for 24 h. Total protein lysates were subjected to immunoblotting. JeKo-1 cells were used as a positive control. **B** JeKo-1 or A20 cells were treated with the indicated doses of pevonedistat for 48 h. Cell proliferation was measured by colorimetric MTS assay. % of viable cells were calculated against untreated controls. **C** A20 lymphoma cells were transplanted into syngeneic recipient mice. Mice were treated with 60 mg/kg pevonedistat or vehicle control for 10 days with or without an anti-CD8 antibody (250 μg i.p. on days 4, 6, 8, and 10 after tumor inoculation). Tumors were measured at the end of the experiment and used for TIL analysis. **D, E** Immune profiles of tumor-infiltrating CD8⁺ and CD4⁺ T cells. **F** PCR products and a representative flow cytometry histogram of WT vs *B2M*^{-/-} A20 cells are shown. **G** A20 *B2M*-KO mice were treated with pevonedistat versus vehicle control as previously (*n* = 6 each). Tumor growth curve is shown. **H** Immune profiles of CD8⁺ and CD4⁺ TILs are shown. Data are mean ± SD. One-way ANOVA was performed for statistical analysis, **p* < 0.05, ****p* < 0.001.

inhibition-induced cytotoxicity of allogeneic T cells (Fig. 5D), suggesting that immunomodulatory effect of pevonedistat is at least in part mediated via HIF-1α.

To further elucidate the role of CRL blockade in HIF-1α upregulation, we generated *UBE2M* knockdown in primary

patient-derived T cells (Fig. 5E). As predicted, *UBE2M* knockdown resulted in upregulation of HIF-1α protein expression, albeit to a lesser degree than pevonedistat treatment. This was likely explained by incomplete knockdown of *UBE2M*. Interestingly, we also observed that treatment with pevonedistat increased HIF-1α

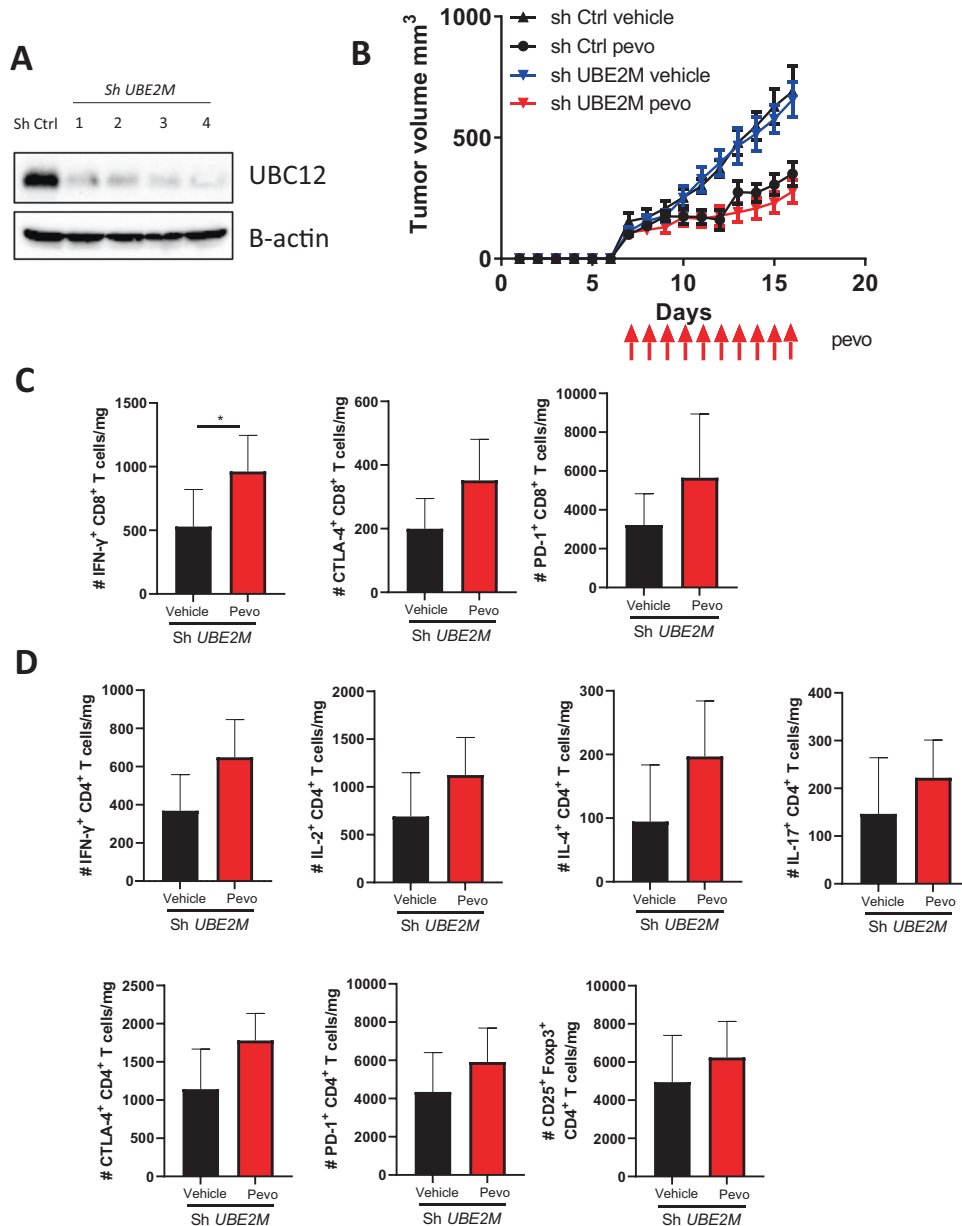


Fig. 4 Therapeutic effect of pevonedistat does not depend on tumor-intrinsic effects. A20 cells were transduced with lentivirus bearing *UBE2M* shRNA and stable knockdown cell lines were selected by puromycin. sh*UBE2M* or control A20 cells were transplanted into syngeneic recipient mice, tumor-bearing mice were randomized into 2 groups and treated with vehicle control or pevonedistat 60 mg/kg for 10 days. **A** Whole-cell lysate proteins from A20 tumors collected at the end of mouse experiment were subjected to immunoblotting. 4 individually obtained cell lines are shown. **B** Tumor growth of A20 lymphoma upon pevonedistat treatment ($n = 6$). **C, D** Immune profiles of CD8⁺ and CD4⁺ TILs. Data are mean \pm SD. * $p < 0.05$.

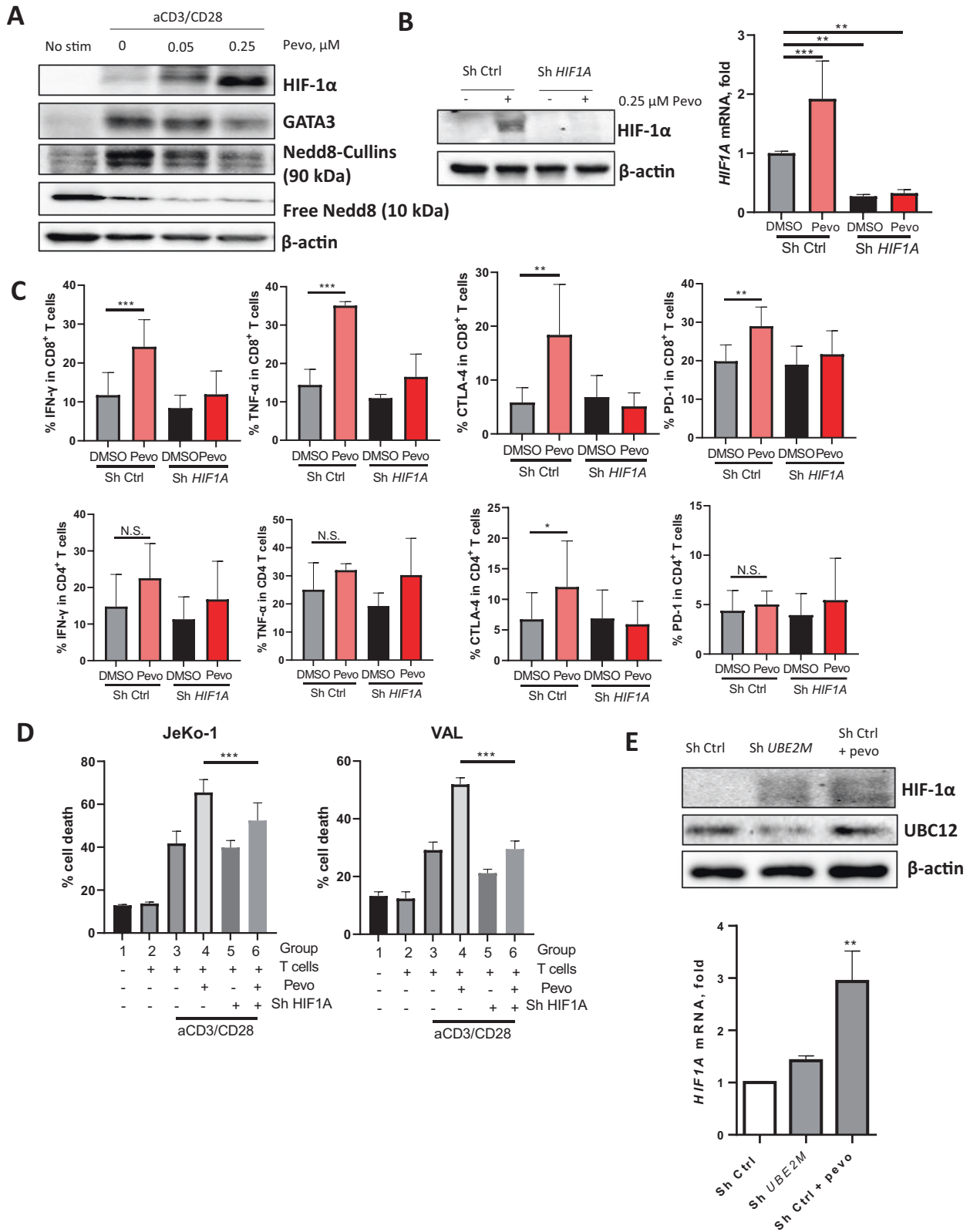
mRNA transcript levels (Fig. 5B), suggesting that pevonedistat mediates HIF-1 α levels via additional mechanisms, not limited to regulation of protein turnover.

NAE inhibition enhances efficacy of PD-1 blockade

We postulated that since NAE inhibition enhances T-cell anti-tumor immunity, pevonedistat may sensitize lymphoid tumors to immune checkpoint inhibitors. While PD-1 inhibition exhibited a partial anti-tumor effect, combined treatment with pevonedistat arrested *in vivo* growth of A20 lymphomas (Fig. 6A). This was accompanied by increased IFN- γ production in both CD8⁺ and CD4⁺ murine TILs (Fig. 6B, C). Moreover, combined treatment upregulated secretion of multiple cytokines by the CD4⁺ TILs (Fig. 6C). As expected, the combination of pevonedistat and

anti-PD-1 had no therapeutic efficacy in A20 *B2M*-KO lymphomas (Supplementary Fig. 7A, C).

Previous studies have shown that pevonedistat may upregulate PD-L1 expression by the tumor cells via MYC oncogene [18, 32]. Consistent with this notion, we found that treatment with pevonedistat upregulated MYC expression, but not IFN- γ , in A20 cells *in vitro* (Supplementary Fig. 7D, E). Furthermore, both *in vitro* and *in vivo* treatment with pevonedistat led to increased PD-L1 expression by A20 cells (Supplementary Fig. 7F), possibly accounting for their sensitization to combined PD-1 blockade. Coupled with the above evidence that inactivation of the neddylation pathway in the tumor does not negatively impact *in vivo* effect of pevonedistat, this supports the idea that immune effects of NAE inhibition likely result from a direct effect on T cells.



Immunomodulatory effect of pevonedistat patients with NHL
 To evaluate relevance of our findings to human disease, we analyzed T cells from patients with NHL who received pevonedistat on the Phase I clinical trial (NCT03479268) [24]. PBMCs were isolated from blood samples collected at baseline (prior to pevonedistat first

dose), and 3 and 24 h after pevonedistat infusion. We observed enhanced IFN- γ secretion in CD4⁺ and CD8⁺ T cells as early as 3 h post infusion (Fig. 7A). The induction of IFN- γ in CD8⁺ T cells persisted for at least 24 h. Meanwhile, expression of either PD-1 or CTLA-4 was not affected by pevonedistat (Fig. 7B). As expected,

Fig. 5 HIF-1 α mediates NAE effect in T cells. Magnetically enriched CD3⁺ cells were activated with 0.5 μ g/mL α CD3/28 for 24 h. **A** Thereafter, stimulation continued in the presence of the indicated doses of pevonedistat or vehicle control for an additional 72 h. Protein expression was quantified by immunoblotting. **B** T cells were transduced by lentivirus bearing with *HIF1A* shRNA (or vector control) overnight. Thereafter, stimulation continued in the presence of 0.25 μ M pevonedistat or vehicle control for an additional 72 h. HIF-1 α expression was quantified by immunoblotting (left) and RT-PCR (right). **C** Expression of IFN γ , TNF α , CTLA-4 and PD-1 was quantified in CD8⁺ T cells by flow cytometry. **D** T cells were stimulated with CD3/28 and treated with pevonedistat as above. The drug was washed off, and T cells were co-cultured with CFSE-labeled JeKo-1 or VAL cells for 48 h. Apoptosis was quantified by flow cytometry using Annexin V/7-AAD. Data are mean \pm SD. One-way ANOVA was performed for statistical analysis, ** p < 0.01, *** p < 0.001. **E** T cells were transduced with *UBE2M* shRNA (or vector control). Thereafter, stimulation continued in the presence of 0.25 μ M pevonedistat or vehicle control for an additional 72 h. HIF-1 α expression was quantified by immunoblotting and RT-PCR.

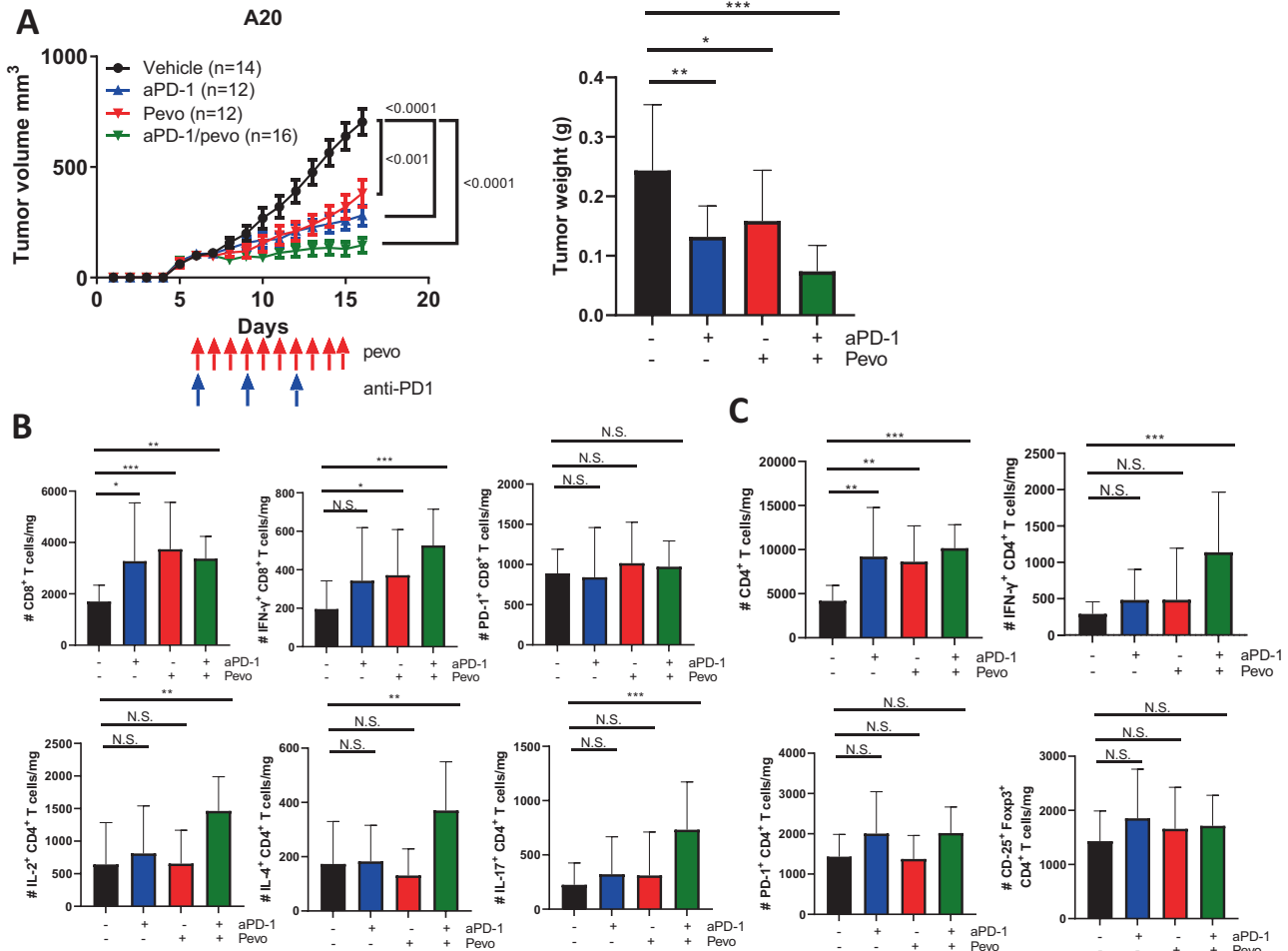


Fig. 6 Combined targeting NAE and PD-1 in A20 lymphoma. **A–C** A20 lymphoma cells were transplanted into syngeneic recipient mice, and tumor-bearing mice were randomized into 4 groups and treated with vehicle control, pevonedistat (as previously), anti-PD-1 antibody (200 μ g/mouse/dose, i.p., on days 6, 9, and 12), or both. Tumors were measured daily and at the end of the experiment (right panel) and subsequently were used for TIL analysis. Immune profiles of CD4⁺ and CD8⁺ TILs are shown. * p < 0.05, ** p < 0.01, *** p < 0.001.

treatment with pevonedistat had no immediate effect on production of other cytokines (Fig. 7C).

Additionally, paired samples from 4 patients with NHL enrolled on the above study were submitted for scRNA-Seq to study the effect of pevonedistat on immune cells. After quality control 2306 (PV7), 4533 (PV14), 7402 (PV23) and 992 cells (PV24) were obtained. In the published analysis, we documented rapid downregulation of NF κ B signaling in malignant B cells following pevonedistat infusion [24]. Here we conducted immune cell population analysis. Between 2 and 6 immune cell types were identified in each patient, including CD4⁺, CD8⁺ T cells, CD16⁺ and CD16⁻ monocytes, B cells and NK cells (Fig. 7D). For each immune cell type, we examined the effect of pevonedistat on the transcriptome across multiple patients. Pathway level analysis

confirmed downregulation of “TNF α signaling via NF κ B” in CD8⁺ T cells, CD16⁺ monocytes and NK cells 24 h post infusion, consistent with our earlier above and the established target of NAE inhibition (data not shown). Meanwhile, “IFN- α response” was upregulated in CD4⁺ and CD8⁺ T cells as early as after 3 h of pevonedistat infusion (Supplementary Fig. 8A). Furthermore, upregulation of IFN- α and IFN- γ response was observed 24 h post infusion in T cells, monocytes and NK cells (Fig. 7E), indicating that pevonedistat triggered interferon signaling and thus reinvigorating T cells responses in vivo. Consistent with known mechanistic effects of pevonedistat, we detected activation of DNA repair pathways across multiple cell types (Supplementary Fig. 8B). We also detected upregulation of HIF-1 α gene signatures in CD4⁺ T cells (Supplementary Fig. 8C).

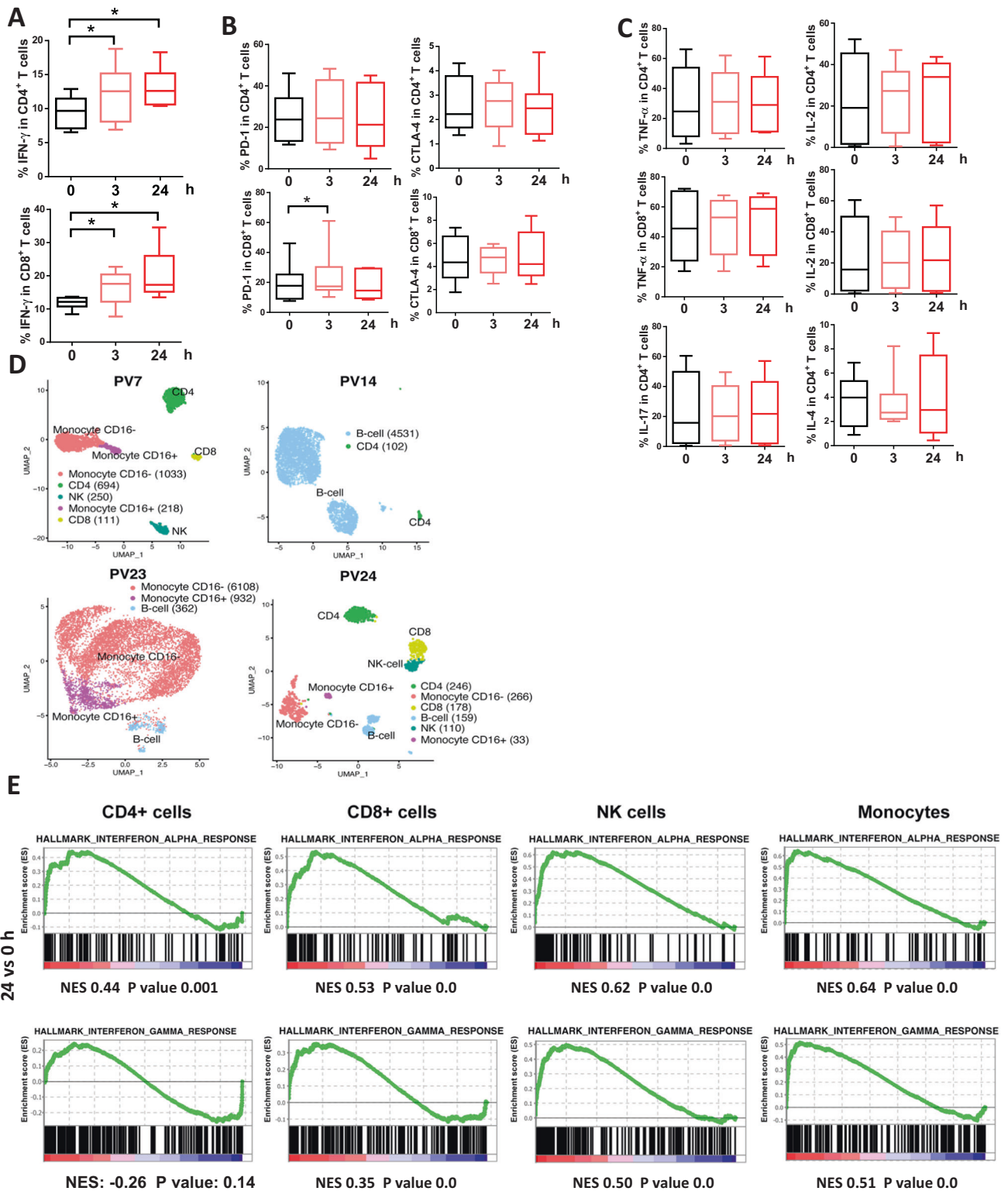


Fig. 7 Clinical effect of pevonedistat in NHL patients. PBMC were collected at baseline and 3 and 24 h post-pevonedistat infusion. For cytokine staining, equal numbers of human PBMC cells were cultured in vitro for 5 h in the presence of PMA, ionomycin and BFA. **A** IFN- γ **B** CTLA-4 and PD-1 and **C** TNF α , IL-2, IL-4 and IL-17 expression was quantified in CD4⁺ or CD8⁺ T cells by flow cytometry. Data are mean \pm SEM, * p < 0.05. **D** UMAP (uniform manifold approximation and projection) visualization of all cells colored by cell type. **E** GSEA (gene set enrichment analysis) plots illustrating the significant enrichment of hallmark IFN- α and IFN- γ response pathways in 24 h post infusion versus baseline in the indicated cell types. The green line represented the enrichment of pathway in the 24 h post infusion group or control baseline group according to gene expression levels, with genes enriched in the 24 h post infusion group shown on the left and genes enriched in the control baseline group shown on the right. NES normalized enrichment score.

Taken together, this data indicate that pharmacologic targeting NAE had a distinct immunomodulatory effect *in vivo*.

DISCUSSION

Here we demonstrate that selective NAEi enhances anti-tumor immunity *in vitro* and in syngeneic lymphoma mouse models. We have previously shown that pevonedistat downmodulated IL-2 production and blunted proliferation of the CD4⁺ T cells derived from patients with CLL [21]. Current *in vitro* analysis uncovered additional effects, demonstrating upregulation of IFN- γ and TNF- α by the TCR-stimulated CD8⁺ cells treated with pevonedistat. Consistent with earlier data, both T-cell subsets showed increased expression of CTLA-4, a checkpoint inhibitor, which could be related to NAEi-mediated downregulation of NFAT and FoxP3 [21, 33, 34].

Importantly, we observed increased *in vitro* cytotoxic effects of the NAEi-conditioned T cells against the lymphoma cell lines, prompting us to investigate pevonedistat effects *in vivo*. Treatment with pevonedistat resulted in delayed progression of A20 lymphoma tumors, associated with increased CD4⁺ and CD8⁺ T-cell infiltration. Furthermore, we have shown that the therapeutic effect of pevonedistat was T-cell-dependent, since (1) depletion of CD8⁺ T cells and (2) genetic knockout of β 2-microglobulin in A20 lymphoma cells fully reversed the anti-tumor effect. Emerging data suggest that neddylation is capable of regulating the tumor microenvironment, including macrophages, dendritic cells, NK cells and T cells [21–23, 35–39].

The evidence of the role of neddylation in T-cell biology remains limited and controversial. Loss of the Nedd8-conjugating enzyme UBC12 in CD4⁺ T cells led to diminished proliferation, skewed T_{H1}/T_{H2} differentiation and reduced cytokine production [36]. Pevonedistat had comparable effects in a malaria murine model, where deficiency of *UBA3*, which encodes the catalytic subunit of the NAE, significantly compromised survival, activation, and proliferation of CD4⁺ T cells and impaired T_{H1}/T_{FH} differentiation [37]. Furthermore, pevonedistat was shown to suppress the ability of dendritic cells to stimulate murine and human allogeneic T-cell responses [40]. However, despite the data regarding the role of neddylation in non-cancer settings, an emerging body of data favors the notion that targeting NAE may ultimately enhance T/NK cell immunity. A recent study has shown that pevonedistat may limit tumor infiltration by the immune suppressor cells, including tumor-associated macrophages and myeloid derived suppressor cells, and promote CD8⁺ T-cell infiltration in lung cancer models [41]. In multiple myeloma models, NAE inhibition upregulated NKG2D ligands, leading to the activation of NK cells [22]. Here we provide evidence that neddylation critically restrains anti-tumor immunity, while its inhibition reverses this effect. This effect is not limited to A20 model, but also occurs in the immunologically “cold” Lewis lung carcinoma. Therefore, it is likely applicable across a spectrum of tumor tissues.

In this study, we observed significant effects of pevonedistat on CD8⁺ T cells. Yet we did not fully elucidate contribution of other cells to anti-tumor immunity. In fact, given our earlier work demonstrating that NAE inhibition suppressed expansion of Treg cells and increased CD4⁺ T-cell polarization towards T_{H1} phenotype *in vitro* and in ova-stimulation model *in vivo* [21], CD4⁺ T cells likely significantly contribute to anti-tumor effect. Ongoing studies should further clarify the interplay between the immune cell fractions upon NAE inhibition.

We further show that pevonedistat cooperates with checkpoint inhibition in the A20 model. Our result is consistent with published reports. As an example, concurrent targeting of NAE and PD-L1 restored anti-tumor immunity in prostate cancer models [42]. Genetic or pharmacologic targeting neddylation has previously been shown to upregulate PD-L1 expression in gliomas via MYC [18, 32]. While here we also found increased PD-L1 expression by A20 cells exposed to pevonedistat, whether the combined effect

was due to inhibiting neddylation in the tumor versus a T-cell-intrinsic effect or modulation of additional immune microenvironment signaling [43], has not been addressed. To this end, McGrail et al. suggested that NAE inhibition may enhance tumor antigenicity. They reported that presence of microsatellite instability (MSI) enhanced tumor cells dependence on neddylation to clear misfolded protein aggregates resulting from destabilizing mutations, leading to immunologic cell death with co-targeting NAE and PD-1 [44]. By contrast, we for the first time demonstrate that immunologic effects of NAEi are fully T-cell-dependent. Genetic abolition of the neddylation pathway in A20 cells did not limit growth of control tumors and, more importantly, did not abolish the anti-tumor effect of pevonedistat. This gives further confidence that the immunomodulatory effect of NAEi will be conserved across multiple tumor types, irrespective of tumor genetic mutations.

The observed immunomodulatory effect of pevonedistat is not entirely surprising given its effect on E3 ligase function. In a recent study, avadomide, a Cereblon E3 ligase modulator, was shown to induce type I and II IFN signaling in T cells, reinvigorating T-cell responses in NHL models [45]. Avadomide promoted T-cell proliferation and chemokine synthesis, upregulated PD-L1 in the immune tumor microenvironment, and stimulated activation of cytotoxic CD8⁺ T cells when combined with anti-PD-L1 antibodies in patient-derived xenograft tumors. The immunomodulatory effect of lenalidomide and other drugs in this class have long been exploited in therapy of hematologic malignancies [46].

How exactly does pevonedistat achieves immunologic effects? Here we have shown that pevonedistat upregulates expression of HIF-1 α , an established CRL protein substrate. In addition to that, we also observed increased *HIF1A* mRNA transcript levels in cells treated with pevonedistat. *HIF1A* knockdown compromised NAE-inhibition mediated T-cell cytotoxicity *in vitro*, indicating that Nedd8-HIF-1 α is a critical pathway that governs immune response. HIF-1 α deficiency has been shown to cause reduced activation and tumor infiltration by the CD8⁺ cytotoxic T cells, leading to compromised tumor cell killing and alteration of tumor vascularization [31]. Furthermore, checkpoint receptor expression (TIM3, PD-1, CTLA-4 and LAG-3), is in part regulated by HIF-1 α [31]. Thus, upregulation of CTLA-4 by pevonedistat in T cells observed by us may also indirectly implicate HIF-1 α signaling pathway as a key NAEi mediator. HIF-1 α turnover is regulated by VHL and mutations in VHL, many occurring in the region interacting with CRLs, disrupt the ubiquitylation of HIF-1 α [47–49]. This mechanism remains an area of active investigation by our group.

Finally, we have shown that some of the effects observed preclinically can be recapitulated in patients with NHL. We used scRNA-Seq technology to demonstrate that patients who received pevonedistat on a clinical trial exhibited disruption in NF κ B signaling and DNA repair pathways, consistent with known targets of NAE inhibition [10]. And yet, a single pevonedistat infusion resulted in upregulated IFN- γ secretion by CD8⁺ T cells, as well as rapid induction of IFN signaling pathways across multiple cell types. Taken together, our preclinical and clinical data strongly suggest that neddylation is an important target which can be exploited to enhance the anti-tumor immunity. Perhaps the future studies should focus on combination strategies where pevonedistat is employed to enhance efficacy of checkpoint inhibitors, bi-specific antibodies or cellular therapies.

DATA AVAILABILITY

The data that support the findings of this study are available from the corresponding author upon reasonable request.

REFERENCES

- Dickinson MJ, Carlo-Stella C, Morschhauser F, Bachy E, Corradini P, Iacoboni G, et al. Glofitamab for relapsed or refractory diffuse large B-cell lymphoma. *N Engl J Med*. 2022;387:2220–31.

2. Kersh AE, Ng S, Chang YM, Sasaki M, Thomas SN, Kissick HT, et al. Targeted therapies: immunologic effects and potential applications outside of cancer. *J Clin Pharmacol*. 2018;58:7–24.
3. Maharaj K, Sahakian E, Pinilla-Ibarz J. Emerging role of BCR signaling inhibitors in immunomodulation of chronic lymphocytic leukemia. *Blood Adv*. 2017;1:1867–75.
4. Lam V, Best S, Kittai A, Orand K, Spurgeon SE, Liu T, et al. Proapoptotic and immunomodulatory effects of SYK inhibitor entospletinib in combination with obinutuzumab in patients with chronic lymphocytic leukaemia. *Br J Clin Pharmacol*. 2022;88:836–41.
5. Ramsay AG, Johnson AJ, Lee AM, Gorgun G, Le Dieu R, Blum W, et al. Chronic lymphocytic leukemia T cells show impaired immunological synapse formation that can be reversed with an immunomodulating drug. *J Clin Invest*. 2008;118:2427–37.
6. Ramsay AG, Evans R, Kiai S, Svensson L, Hogg N, Gribben JG. Chronic lymphocytic leukemia cells induce defective LFA-1-directed T-cell motility by altering Rho GTPase signaling that is reversible with lenalidomide. *Blood*. 2013;121:2704–14.
7. Damgaard RB. The ubiquitin system: from cell signalling to disease biology and new therapeutic opportunities. *Cell Death Differ*. 2021;28:423–6.
8. Petroski MD, Deshaies RJ. Function and regulation of cullin-RING ubiquitin ligases. *Nat Rev Mol Cell Biol*. 2005;6:9–20.
9. Watson IR, Irwin MS, Ohh M. NEDD8 pathways in cancer, *Sine Quibus Non*. *Cancer Cell*. 2011;19:168–76.
10. Soucy TA, Smith PG, Milhollen MA, Berger AJ, Gavin JM, Adhikari S, et al. An inhibitor of NEDD8-activating enzyme as a new approach to treat cancer. *Nature*. 2009;458:732–6.
11. Shah JJ, Jakubowiak AJ, O'Connor OA, Orlowski RZ, Harvey RD, Smith MR, et al. Phase I study of the novel investigational NEDD8-activating enzyme inhibitor pevonedistat (MLN4924) in patients with relapsed/refractory multiple myeloma or lymphoma. *Clin Cancer Res*. 2016;22:34–43.
12. Swords RT, Erba HP, DeAngelo DJ, Bixby DL, Altman JK, Maris M, et al. Pevonedistat (MLN4924), a First-in-Class NEDD8-activating enzyme inhibitor, in patients with acute myeloid leukaemia and myelodysplastic syndromes: a phase 1 study. *Br J Haematol*. 2015;169:534–43.
13. Milhollen MA, Traore T, Adams-Duffy J, Thomas MP, Berger AJ, Dang L, et al. MLN4924, a NEDD8-activating enzyme inhibitor, is active in diffuse large B-cell lymphoma models: rationale for treatment of NF- κ B-dependent lymphoma. *Blood*. 2010;116:1515–23.
14. Godbersen JC, Humphries LA, Danilova OV, Kebbekus PE, Brown JR, Eastman A, et al. The Nedd8-activating enzyme inhibitor MLN4924 thwarts microenvironment-driven NF- κ B activation and induces apoptosis in chronic lymphocytic leukemia B cells. *Clin Cancer Res*. 2014;20:1576–89.
15. Gu Y, Kaufman JL, Bernal L, Torre C, Matulis SM, Harvey RD, et al. MLN4924, a NAE inhibitor, suppresses AKT and mTOR signaling via upregulation of REDD1 in human myeloma cells. *Blood*. 2014;123:3269–76.
16. Luo Z, Yu G, Lee HW, Li L, Wang L, Yang D, et al. The Nedd8-activating enzyme inhibitor MLN4924 induces autophagy and apoptosis to suppress liver cancer cell growth. *Cancer Res*. 2012;72:3360–71.
17. Jia X, Li C, Li L, Liu X, Zhou L, Zhang W, et al. Neddylation inactivation facilitates FOXO3a nuclear export to suppress estrogen receptor transcription and improve fulvestrant sensitivity. *Clin Cancer Res*. 2019;25:3658–72.
18. Zhou S, Zhao X, Yang Z, Yang R, Chen C, Zhao K, et al. Neddylation inhibition upregulates PD-L1 expression and enhances the efficacy of immune checkpoint blockade in glioblastoma. *Int J Cancer*. 2019;145:763–74.
19. Paiva C, Godbersen JC, Berger A, Brown JR, Danilov AV. Targeting neddylation induces DNA damage and checkpoint activation and sensitizes chronic lymphocytic leukemia B cells to alkylating agents. *Cell Death Dis*. 2015;6:e1807.
20. Paiva C, Godbersen JC, Rowland T, Danilova OV, Danes C, Berger A, et al. Pevonedistat, a Nedd8-activating enzyme inhibitor, sensitizes neoplastic B-cells to death receptor-mediated apoptosis. *Oncotarget*. 2017;8:21128–39.
21. Best S, Lam V, Liu T, Bruss N, Kittai A, Danilova OV, et al. Immunomodulatory effects of pevonedistat, a NEDD8-activating enzyme inhibitor, in chronic lymphocytic leukemia-derived T cells. *Leukemia*. 2021;35:156–68.
22. Petillo S, Capuano C, Molfetta R, Fionda C, Mekhloufi A, Pighi C, et al. Immunomodulatory effect of NEDD8-activating enzyme inhibition in Multiple Myeloma: upregulation of NKG2D ligands and sensitization to Natural Killer cell recognition. *Cell Death Dis*. 2021;12:836.
23. Wang X, Best S, Danilov AV. Neddylation and anti-tumor immunity. *Oncotarget*. 2021;12:2227–30.
24. Torka P, Kambhampati S, Chen L, Wang X, Chen C, Vuong D, et al. Pevonedistat, a Nedd8-activating enzyme inhibitor, in combination with ibrutinib in patients with relapsed/refractory B-cell non-Hodgkin lymphoma. *Blood Cancer J*. 2023;13:9.
25. Knorr KL, Schneider PA, Meng XW, Dai H, Smith BD, Hess AD, et al. MLN4924 induces Noxa upregulation in acute myelogenous leukemia and synergizes with Bcl-2 inhibitors. *Cell Death Differ*. 2015;22:2133–42.
26. Torka P, Mavis C, Kothari S, Belliotti S, Gu J, Sundaram S, et al. Pevonedistat, a NEDD8-activating enzyme inhibitor, induces apoptosis and augments efficacy of chemotherapy and small molecule inhibitors in pre-clinical models of diffuse large B-cell lymphoma. *EJHaem*. 2020;1:122–32.
27. Kittai AS, Danilova OV, Lam V, Liu T, Bruss N, Best S, et al. NEDD8-activating enzyme inhibition induces cell cycle arrest and anaphase catastrophe in malignant T-cells. *Oncotarget*. 2021;12:2068–74.
28. Wang X, Waschke BC, Woolaver RA, Chen Z, Zhang G, Piscopio AD, et al. Histone deacetylase inhibition sensitizes PD1 blockade-resistant B-cell lymphomas. *Cancer Immunol Res*. 2019;7:1318–31.
29. Song N, Cao C, Tang YM, Bi LY, Jiang Y, Zhou YS, et al. The ubiquitin ligase SCFFBXW7 alpha promotes GATA3 degradation. *J Cell Physiol*. 2018;233:2366–77.
30. Gibson HM, Mishra A, Chan DV, Hake TS, Porcu P, Wong HK. Impaired proteasome function activates GATA3 in T cells and upregulates CTLA-4: relevance for Sezary syndrome. *J Invest Dermatol*. 2013;133:249–57.
31. Palazon A, Tyrakis PA, Macias D, Velica P, Rundqvist H, Fitzpatrick S, et al. An HIF-1 alpha/VEGF-A axis in cytotoxic T cells regulates tumor progression. *Cancer Cell*. 2017;32:669.
32. Filippova N, Yang X, An Z, Nabors LB, Pereboeva L. Blocking PD1/PDL1 interactions together with MLN4924 therapy is a potential strategy for glioma treatment. *J Cancer Sci Ther*. 2018;10:190–7.
33. Gibson HM, Hedgcock CJ, Aufiero BM, Wilson AJ, Hafner MS, Tsokos GC, et al. Induction of the CTLA-4 gene in human lymphocytes is dependent on NFAT binding the proximal promoter. *J Immunol*. 2007;179:3831–40.
34. Chen C, Rowell EA, Thomas RM, Hancock WW, Wells AD. Transcriptional regulation by Foxp3 is associated with direct promoter occupancy and modulation of histone acetylation. *J Biol Chem*. 2006;281:36828–34.
35. Zhou L, Jiang Y, Luo Q, Li L, Jia L. Neddylation: a novel modulator of the tumor microenvironment. *Mol Cancer*. 2019;18:77.
36. Jin HS, Liao L, Park Y, Liu YC. Neddylation pathway regulates T-cell function by targeting an adaptor protein Shc and a protein kinase Erk signaling. *Proc Natl Acad Sci USA*. 2013;110:624–9.
37. Cheng Q, Liu J, Pei Y, Zhang Y, Zhou D, Pan W, et al. Neddylation contributes to CD4+ T cell-mediated protective immunity against blood-stage Plasmodium infection. *PLoS Pathog*. 2018;14:e1007440.
38. Mathewson ND, Fujiwara H, Wu SR, Toubai T, Oravec-Wilson K, Sun Y, et al. SAG/Rbx2-dependent neddylation regulates T-cell responses. *Am J Pathol*. 2016;186:2679–91.
39. Friend SF, Peterson LK, Treacy E, Stefanski AL, Sosinowski T, Pennock ND, et al. The discovery of a reciprocal relationship between tyrosine-kinase signaling and cullin neddylation. *PLoS ONE*. 2013;8:e75200.
40. Mathewson N, Toubai T, Kapeles S, Sun Y, Oravec-Wilson K, Tamaki H, et al. Neddylation plays an important role in the regulation of murine and human dendritic cell function. *Blood*. 2013;122:2062–73.
41. Zhou L, Jiang Y, Liu X, Li L, Yang X, Dong C, et al. Promotion of tumor-associated macrophages infiltration by elevated neddylation pathway via NF- κ B-CCL2 signaling in lung cancer. *Oncogene*. 2019;38:5792–804.
42. Zhang J, Bu X, Wang H, Zhu Y, Geng Y, Nihira NT, et al. Cyclin D-CDK4 kinase destabilizes PD-L1 via cullin 3-SPOP to control cancer immune surveillance. *Nature*. 2018;553:91–5.
43. Tang H, Liang Y, Anders RA, Taube JM, Qiu X, Mulgaonkar A, et al. PD-L1 on host cells is essential for PD-L1 blockade-mediated tumor regression. *J Clin Invest*. 2018;128:580–8.
44. McGrail DJ, Garnett J, Yin J, Dai H, Shih DJH, Lam TNA, et al. Proteome instability is a therapeutic vulnerability in mismatch repair-deficient cancer. *Cancer Cell*. 2020;37:371.
45. Ioannou N, Hagner PR, Stokes M, Gandhi AK, Apollonio B, Fanous M, et al. Triggering interferon signaling in T cells with avadomide sensitizes CLL to anti-PD-L1/PD-1 immunotherapy. *Blood*. 2021;137:216–31.
46. Ioannou N, Jain K, Ramsay AG. Immunomodulatory drugs for the treatment of B cell malignancies. *Int J Mol Sci*. 2021;22:8572.
47. Yu F, White SB, Zhao Q, Lee FS. HIF-1alpha binding to VHL is regulated by stimulus-sensitive proline hydroxylation. *Proc Natl Acad Sci USA*. 2001;98:9630–5.
48. Kamura T, Sato S, Iwai K, Czyzyk-Krzeska M, Conaway RC, Conaway JW. Activation of HIF1alpha ubiquitination by a reconstituted von Hippel-Lindau (VHL) tumor suppressor complex. *Proc Natl Acad Sci USA*. 2000;97:10430–5.
49. Kaelin WG Jr. Molecular basis of the VHL hereditary cancer syndrome. *Nat Rev Cancer*. 2002;2:673–82.

ACKNOWLEDGEMENTS

This study was supported by the NCI 1R01CA244576 and by a grant from Takeda Development Center Americas Inc. (to AVD). AVD is a Leukemia and Lymphoma Society Scholar in Clinical Research (#2319-19).

AUTHOR CONTRIBUTIONS

XW, ZX, NP, AB, LW and AVD designed research. CC, DV, SRR, VL, CR, PT and FHI and AVD performed research and analyzed data. JHW, PT, FHI, LW and TS contributed vital reagents. All authors wrote and edited the paper.

FUNDING

Open access funding provided by SCELCC, Statewide California Electronic Library Consortium.

COMPETING INTERESTS

AVD has received consulting fees from Abbvie, AstraZeneca, Bayer Oncology, BeiGene, Bristol Meyers Squibb, Genentech, GenMab, Incyte, Janssen, Lilly Oncology, Nurix, Oncovalent, Pharmacyclics and TG Therapeutics and has ongoing research funding from Abbvie, AstraZeneca, Bayer Oncology, Bristol Meyers Squibb, Cyclacel, MEI Pharma, Nurix and Takeda Oncology. PT has received consulting fees from ADC Therapeutics, Genentech and TG Therapeutics.

ADDITIONAL INFORMATION

Supplementary information The online version contains supplementary material available at <https://doi.org/10.1038/s41375-023-01889-x>.

Correspondence and requests for materials should be addressed to Alexey V. Danilov.

Reprints and permission information is available at <http://www.nature.com/reprints>

Publisher's note Springer Nature remains neutral with regard to jurisdictional claims in published maps and institutional affiliations.



Open Access This article is licensed under a Creative Commons Attribution 4.0 International License, which permits use, sharing, adaptation, distribution and reproduction in any medium or format, as long as you give appropriate credit to the original author(s) and the source, provide a link to the Creative Commons license, and indicate if changes were made. The images or other third party material in this article are included in the article's Creative Commons license, unless indicated otherwise in a credit line to the material. If material is not included in the article's Creative Commons license and your intended use is not permitted by statutory regulation or exceeds the permitted use, you will need to obtain permission directly from the copyright holder. To view a copy of this license, visit <http://creativecommons.org/licenses/by/4.0/>.

© The Author(s) 2023